Morphological and chemical variability of colloids in the Almeria-Oran Front in the eastern Alboran Sea (SW Mediterranean Sea)

Hélène Grout, Richard Sempere, Antoine Thill, Anthony Calafat, Louis Prieur, Miquel Canals

Grout, H., Sempéré, R., Thill, A., Calafat, A., Prieur, L., Canals, M., (2001) Morphological and chemical variability of colloids in the Almeria-Oran Front in the eastern Alboran Sea (SW Mediterranean Sea) : evidence by means of analytical electron microscopy. Limnology and Oceanography. 46 : 1347-1357. doi.org/10.4319/lo.2001.46.6.1347

Morphological and chemical variability of colloids in the Almeria–Oran Front in the eastern Alboran Sea (SW Mediterranean Sea)

H. Grout
GRC Geociències Marines, Universitat de Barcelona, Campus de Pedralbes, 08071 Barcelona, Spain

R. Sempere[1]
Laboratoire de Microbiologie Marine, CNRS/INSU, UMR 6117, Case 907, Centre d'Océanologie de Marseille, Campus de Luminy, F13 288 Marseille Cedex 9, France

A. Thill
CEREGE, Europôle Méditerranéen de l'Arbois, BP 80, 13545 Aix-en-Provence, France

A. Calafat
GRC Geociències Marines, Universitat de Barcelona, Campus de Pedralbes, 08071 Barcelona, Spain

L. Prieur
Laboratoire de Physique et Chimie Marines, Observatoire Océanologique, INSU/CNRS, ESA7077, BP 08, F06230 Villefranche-sur-Mer, France

M. Canals
GRC Geociències Marines, Universitat de Barcelona, Campus de Pedralbes, 08071 Barcelona, Spain

Abstract

Across the different water types (Mediterranean, Frontal, and Atlantic waters) in the Almeria–Oran Front (Eastern Alboran Sea, SW Mediterranean Sea), we determined organic carbon in the particulate (60–0.2 μm), colloidal (0.2 μm–1,000 Da) and dissolved (<1,000 Da) fractions. The morphological and chemical variability of colloids was studied by means of analytical electron microscopy. Particulate and colloidal organic fractions accounted for 6 to 9% and 1 to 12%, respectively, of the total organic carbon. Visual examination of colloids revealed three morphologically and chemically differentiated morphotypes (globules, aggregates of rounded entities, and spherulitic aggregates) whose distribution, abundance, and chemical composition vary with the depth and between water types. Globules dominated 5 m deep at all stations; always contained Ca, P, S, and Cl; and were marked by the presence of other elements such as Si, Fe, or Mg depending on the water type. By contrast, at 40 m deep, Mediterranean, Frontal, and Atlantic waters were characterized by different morphotypes: Fe-P–enriched aggregates of rounded entities in Mediterranean waters; globules with variable abundances of Si, Fe, Ca, P, S and Cl in Frontal waters; and Mg-rich spherulitic aggregates in Atlantic waters. These morphological and chemical differences in colloids across the front raise questions about their origin, their aggregation, and the availability of elements for biological activity.

There has been increasing interest in studying marine colloids in recent years. They play an important role in chemical partitioning between phases, mobilization and transport of metals and organic contaminants, and bioavailability of chemical species (Guo and Santschi 1997 and references therein). Colloids are highly abundant in seawater (Koike et al. 1990; Wells and Goldberg 1994; Santschi et al. 1998) and form a significant fraction of the dissolved organic carbon pool. At least some fractions of the colloidal material are thought to be labile and rapidly cycled in the water column; hence, colloids may be a key to understanding the potentially dynamic nature of organic carbon cycling (Amon and Benner 1994). The aggregation of colloids into settling particles is believed to be an important mechanism in the downward transport of organic carbon and surface-reactive chemicals in the ocean (Baskaran et al. 1992; Wells and Goldberg 1993; Moran et al. 1996). In addition, colloids are a component of the matrix of the marine snow particles (Leppard et al. 1996).

[1] Corresponding author (sempere@com.univ-mrs.fr).

Acknowledgments

The authors thank the crew of the R/V *L'Atalante* and acknowledge J. Y. Bottero for the facilities given for ultracentrifugation. We are particularly grateful to one anonymous reviewer, to C. Parron, D. Perret, and M. I. Scranton for helpful comments and improvement of the manuscript, and to J. Sanderson for English revision of the manuscript. We thank the Serveis Científico-Tècnics, University of Barcelona, for allowing us to use their electron microscope. This work is supported by a TMR grant (ERBFMBICT961519), MTPII-MATER project (MAS3-CT96-0051) of the European Community and CNRS/INSU, and France–JGOFS Almofront project. GRC Marine Geosciences is supported by the Generalitat Catalan Autonomous Government grant 1997SGR-80.

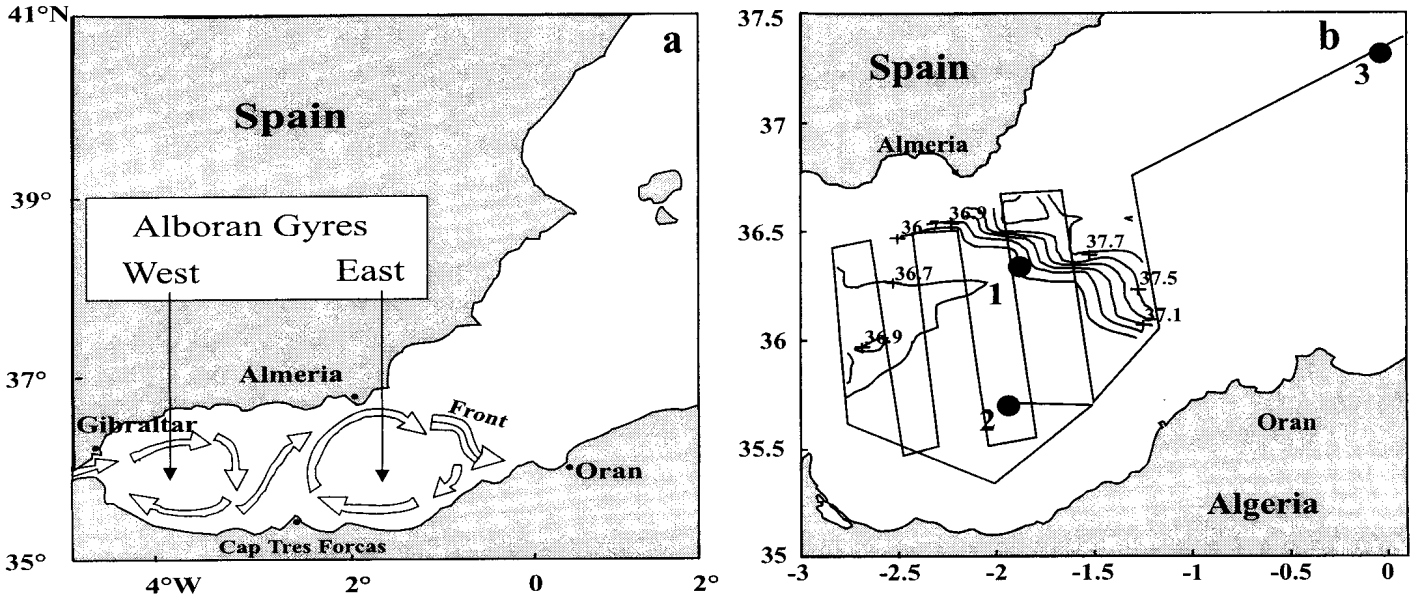

Fig. 1. (a) Map of the southwestern Mediterranean Sea with a schematic depiction of surface water flow of modified Atlantic water from the Strait of Gibraltar, through the Alboran Sea, and as it forms the Almeria–Oran Front. (b) Location of the sampling sites in the Almeria–Oran Front: Site 1, Frontal waters; Site 2, Atlantic waters; Site 3, Mediterranean waters.

The structure of colloids has been used to indicate their origin (Leppard 1997) and to provide information about their role in aquatic systems (Wilkinson et al. 1997), but neither their exact chemical composition nor their morphological characteristics are precisely known because of instrumental and procedural limitations, especially in the smallest fractions. Transmission electron microscopy (TEM) has proven to be a powerful tool for the determination of colloid characteristics such as size, morphology, porosity, degree of aggregation, and crystallinity. TEM resolution permits analyses down to the nanometer range, and in combination with energy-dispersive spectroscopy (EDS), TEM can provide elemental analyses of colloids for a large range of elements. To our knowledge, studies that take both the morphologies and the chemical nature of marine colloids systematically into account are extremely rare. The literature mainly reports the different morphologies encountered (Wells and Goldberg 1994; Leppard et al. 1997). Thus, the colloidal pool in marine environments is morphologically and chemically largely uncharacterized.

The Eastern Alboran Sea (SW Mediterranean Sea) is especially appropriate to investigate the subject because the Almeria–Oran Front (AOF) contains surface Atlantic water over saltier and denser Mediterranean waters. Surficial circulation in the Alboran Sea is dominated by a strong jet of Atlantic water entering through the Strait of Gibraltar (Arnone et al. 1990; Prieur and Sournia 1994). The juxtaposition of the Mediterranean and the Atlantic waters results in a persistent density front (Fig. 1), which is well marked by a strong surface salinity gradient. This feature has repeatedly been shown to be associated with high (sometimes very high) phytoplankton standing stocks and production (references in Videau et al. 1994). The aim of this paper is to describe the variability in composition, structure, morphology, and size of colloidal materials in the different water masses associated with the AOF as revealed by TEM.

Table 1. Characteristics of the surface water types in the Almeria–Oran Front.

Water type	Position	Temperature (°C)	Salinity	Density (kg m^{-3})	Isopycnal 28 depth (m)
Mediterranean	00°03′W 37°20.00′N	17.40	37.59	27.41	35
Frontal	1°53.84′W 36°18.97′N	16.22	36.86	27.13	60
Atlantic	1°56.00′W 35°43.42′N	18.11	36.62	26.49	180

Material and methods

Field study—Seawater samples were collected crossing the Almeria–Oran Front during the first leg of the cruise Almofront 2 carried out in November–December 1997 onboard R/V *L'Atalante*. Three stations were chosen to represent the three main parts of the frontal structure: Mediterranean, Frontal, and Atlantic waters. Frontal water (Site 1 in Fig. 1b) was located near the surface salinity front in the main jet of inflowing Atlantic water with surface salinity around 36.90 (Table 1). The salinity map in Fig. 1b was made with a Thermosalinograph Seacat SBE 21. Using 75-kHz RDI acoustic doppler current profiler (ADCP) measurements, the Atlantic jet was found to surround a well-shaped anticyclonic eddy. Site 2 was located south of the jet and was representative of Atlantic waters, with salinity <36.70. The depth of the isopycnal 28 kg m^{-3} was 60 m, which is representative of the interface between Atlantic and Mediterranean waters. The frontal station was very close to the

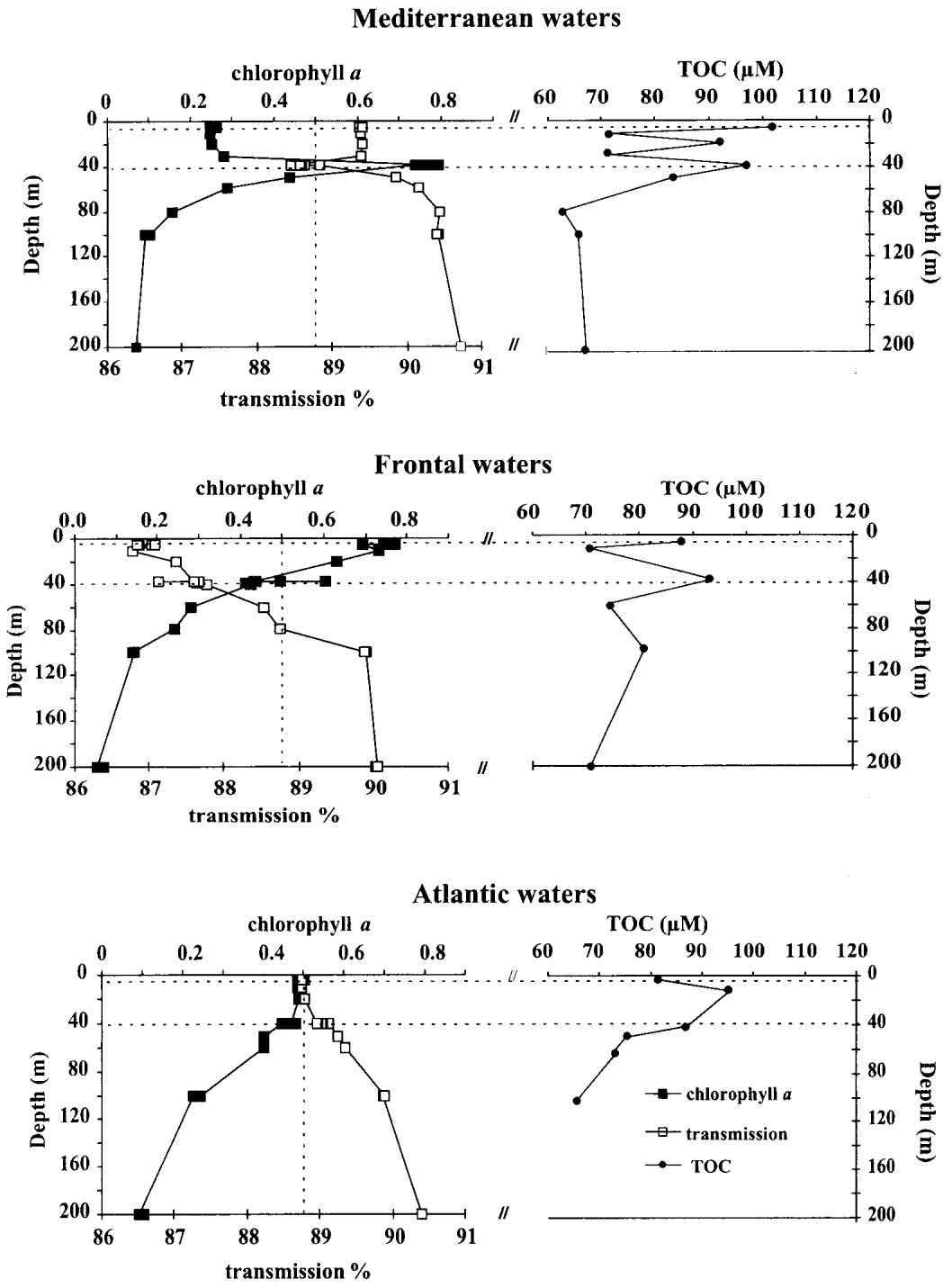

Fig. 2. Chlorophyll *a* and transmission and TOC profiles in Mediterranean, Frontal, and Atlantic waters of the Almeria–Oran Front. The horizontal dashed lines indicate the sampling depth for colloid determinations.

surface salinity front, and Site 2 was in the center part of the eddy. Site 3 was located away from the frontal system proper and was occupied by Mediterranean waters of salinity >37.40.

Sampling and filtration—Water samples were collected with Niskin bottles (fitted with steel closure springs) mounted on a Sea-Bird SBE 09 + conductivity–temperature–depth (CTD) rosette from two depths corresponding to the surface waters (~5 m) and the deep chlorophyll maximum (DCM) at Sta. 3. In order to allow comparison between stations despite the absence of a DCM (Fig. 2), the same two sampling depths were used at the other two stations. Seawater was transferred from the Niskin bottles to 20-L glass bottles using Teflon tubing equipped with a 60-µm mesh net to remove larger organisms and particles. All glass bottles and vials were precombusted for 6 h at 450°C prior to use. Samples were immediately filtered and ultrafiltered using a

Table 2. Organic carbon concentrations (μM) in <1,000-Da, 60–0.2-μm, and 0.2-μm to 1,000-Da size fractions. Mass balances expressed as percentage of initial organic carbon and concentration factor (CF) for the 0.2-μm and 1,000-Da membranes.

	Organic C (μM)			% recovery	CF	% recovery	CF
	<1,000 Da	60–0.2 μm	0.2 μm–1,000 Da	0.2 μm	0.2 μm	1,000 Da	1,000 Da
Mediterranean water							
5 m	68	4	2	108	36	111	33
40 m	56	6	8	116	35	114	36
Frontal water							
5 m	67	7	5	110	34	101	33
40 m	68	6	5	104	33	97	35
Atlantic water							
5 m	83	8	0.8	103	36	101	35
40 m	67	5	3	115	34	105	34

Sartorius cross-flow ultrafiltration (CFF) system equipped first with a 200-nm polysulfone cartridge and then with a 1,000-Da polysulfone cartridge to concentrate the colloids. The cutoff given for both membranes are those given by the manufacturer. The CFF unit also included a peristaltic pump, Teflon tubing, and glass bottles (for the retentate and permeate fractions). Before ultrafiltration, the whole system, including membranes and tubing, was thoroughly cleaned in the laboratory by a series of rinses: 2% NaOH, 0.1% H_3PO_4, and ultrapure water from a Millipore purification unit. Membranes were also cleaned by the same protocol between steps of sample filtration (the cleaning processing time was about 24 h). All ultrafiltrations were carried out onboard immediately after sample collection in a cool room at 16°C over ~24 to 36 h. Five size fractions were obtained: >60 μm, 60–0.2 μm, <0.2 μm, 0.2 μm–1,000 Da, and <1,000 Da. By definition, the 60–0.2-μm fraction contained particulate material, the 0.2-μm to 1,000-Da fraction contained the colloidal material, both the <0.2-μm and <1,000-Da fractions were permeates, and the <1,000-Da fraction was considered to be the dissolved fraction.

Before and after each filtration and ultrafiltration, aliquots for organic carbon analyses were taken from all fractions in duplicate, including initial solutions, permeates, and retentates, using precombusted Pasteur pipettes. They were placed in precombusted 12-ml glass vials in a laminar flow airbench. These aliquots were poisoned with $HgCl_2$ (final concentration 10 mg L^{-1}), covered with a Teflon-lined screw cap, and stored in the dark. For electron microscopic observations, 60 ml of each fraction were collected into polyethylene bottles that had previously been rinsed three times with distilled water, once with 10% HCl solution, and three times with ultrapure water. The organic carbon blank of the 0.2-μm membrane was negligible for both permeate and retentate, whereas those of the 1,000-Da membrane was negligible for retentate and about 3 μM for permeate. The blank, which was determined by ultrafiltration of Milli-Q water, was found to be close to that determined by ultrafiltration of artificial water. This value was subtracted from the values presented here.

Colloidal organic carbon (COC) was calculated (after volume corrections) as the difference between total organic carbon $(TOC)_{concentrate}$ and $TOC_{ultrafiltrate}$. Mass balances (or recovery) were calculated on the samples as percent $TOC_{initial}$ = $[100 \times (TOC_{colloidal} + TOC_{permeate})/TOC_{initial}]$ and ranged from 103 to 116% and from 97 to 114% for the 0.2-μm and 1,000-Da membrane, respectively (Table 2). Recoveries >100% indicate contamination, whereas recoveries <100% indicate loss of TOC during ultrafiltration. The concentration factor ranged from 33 to 36 (Table 2). Although we do not have additional information, class shifting during CFF processing cannot be ruled out.

Vertical profiles of temperature, salinity, density, chlorophyll *a* (Chl *a*) fluorescence (Chelsea fluorometer) and beam attenuation coefficient (Seatech transmissiometer) were recorded at each station down to 200 m. The fluorometer was calibrated in terms of Chl *a* by determination of the pigment concentration by high-performance liquid chromatography.

Analysis of organic carbon—The five size fractions were analyzed for organic carbon content by high temperature combustion (HTC) with a Shimadzu TOC-5000 analyzer (Dafner et al. 1999). Uncertainty in analyses was ±2% based on the uncertainty in the slope of the standard curve. Repeated analysis of low carbon water (provided by J. H. Sharp, University of Delaware) and freshly produced Milli-Q water indicated that the instrument blank ranged from 5 to 10 μM C (average 9 ± 2 μM C). The instrument blank was subtracted from all organic carbon values.

Transmission electron microscopy and EDS—TEM specimens were prepared from ultrafiltration fractions. Colloids were deposited directly by ultracentrifugation on 200-mesh Cu grids (collodion coated, carbon covered) precoated with 5 μl of a hydrophilic resin (Nanoplast FB 101, Frösch and Westphal 1989) and modified by Wilkinson et al. (1995), Grout and Parron (1997), and Grout et al. (1999). The hydrophilic resin preserves fragile structures without the dehydration steps that are generally used in TEM. The sample (15 ml) was ultracentrifuged at 25,000 rpm for 16 h at 10°C using a Sorvall® UltraPro™ 80 ultracentrifuge and a swinging-buckets rotor. After centrifugation, grids were carefully removed, rinsed for at least 1 min with ultrapure water in order to eliminate salts, and placed on Whatman paper in a petri dish for 24 h at room temperature for drying. To check the images for artifacts and reproducibility, a minimum of three specimen grids was prepared and observed for each TEM sample. Microscope fields ranging in magnification

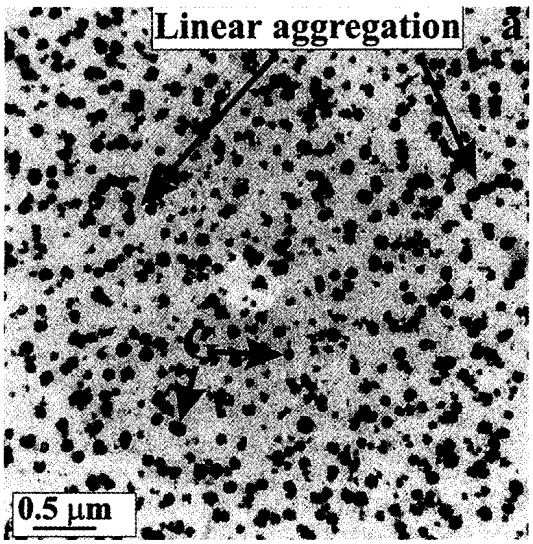

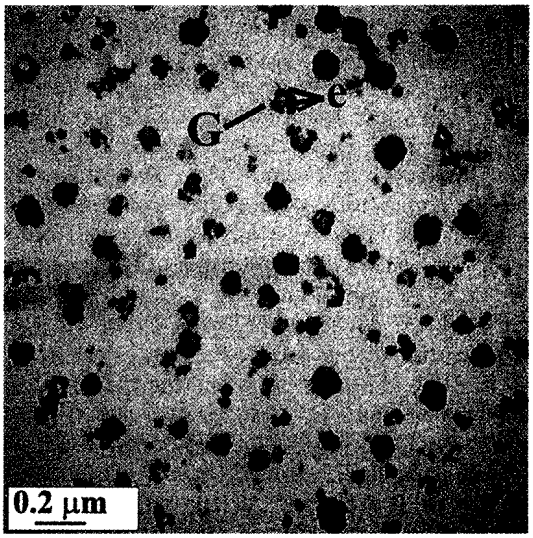

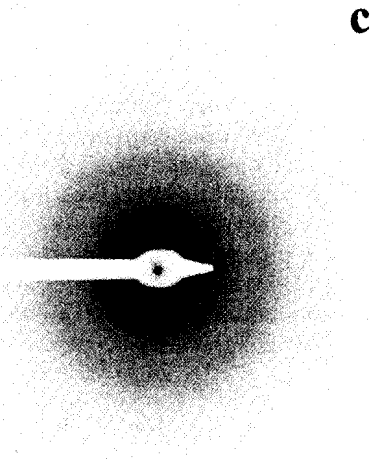

from ×6,000 to ×110,000 were selected from different specimen grid openings and photographed. TEM imaging was performed with a Hitachi H800MET microscope working at 200 kV. The elemental composition of colloids was determined by EDS with a Kevex 8000 Delta class detector. The detector included a mode quantum ultrathin window, resolution FWHM K(α) Mn 152 eV, with Be window of thickness 7 μm, probe size around 50 nm, beam–sample incidence angle of 20°, and X-ray emergence slit angle of 68°. TEM-EDS spectra of individual particles were recorded in the 0–10 keV region. The quantity of each element detected in colloids by EDS for the blank (including CFF runs and TEM grid preparation) represented less than 1% of the quantity of that element detected in seawater samples. Blank levels have been subtracted from the results presented here.

Calculation of fractal dimension—After photography, TEM image analysis was used to determine the fractal dimension of the colloidal aggregates observed as described in detail in Zhang and Buffle (1996). Because the TEM images are two-dimensional projections of three-dimensional objects, methods based on image analysis are useful only for relatively loose aggregates that have a fractal dimension lower than two (Weitz and Huang 1984; Tence et al. 1986). The fractal dimension (df) of the aggregate was obtained using a scaling relationship between mass and radius of the deposited aggregates. First, on the original gray scale pictures, small regions of size 20 by 20 pixels without particles were selected to estimate the background gray scale level. Then a threshold value of twice the background level was applied to the 1,024 by 1,024 TEM images (or on 256 by 256 parts) to produce binary pictures. Concentric circles were drawn from a given origin placed on a particle in the central region of the aggregate. Then, the number of black pixels within each circle was summed. The mass of the aggregates was assumed to be proportional to the number of pixels. Because the mass of a fractal aggregate within a circle of size r is proportional to r^{df}, a value of the fractal dimension was obtained from a log-log plot of dark pixel number versus circle radius.

Results and discussion

Biological characteristics of the different water masses—Vertical profiles of transmission and Chl *a* (Fig. 2) are inversely correlated, showing that most of the particles >1 μm encountered in the water column correspond to phytoplankton. Near the surface (5 m), Mediterranean waters were characterized by a low Chl *a* content (~0.25 mg m^{-3}), whereas in Frontal waters, the concentration was highest (~0.80 mg m^{-3}). Atlantic waters had an intermediate Chl *a* content (0.50 mg m^{-3}). At 40 m, the Chl *a* at the deep chlorophyll maximum (DCM) was highest in Mediterranean waters

←

Fig. 3. TEM images of globule (G) morphotype as described in the text. (a) Some globules contain linear aggregates. (b) Each globule is made up of several components (e). (c) Typical microdiffraction picture of the globules.

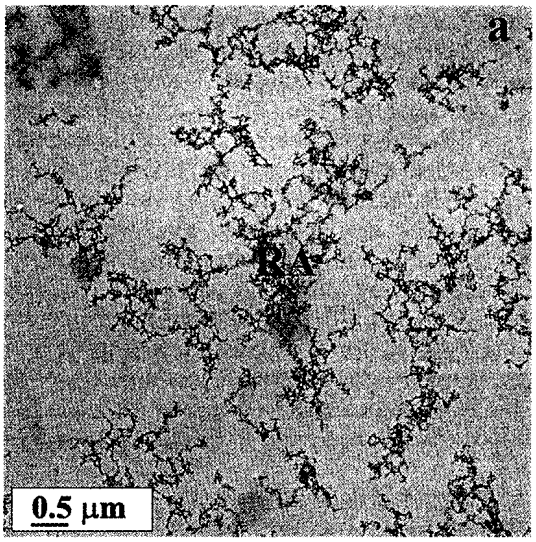

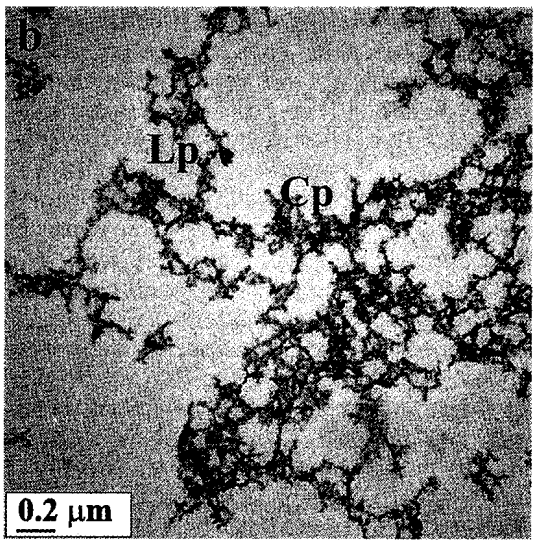

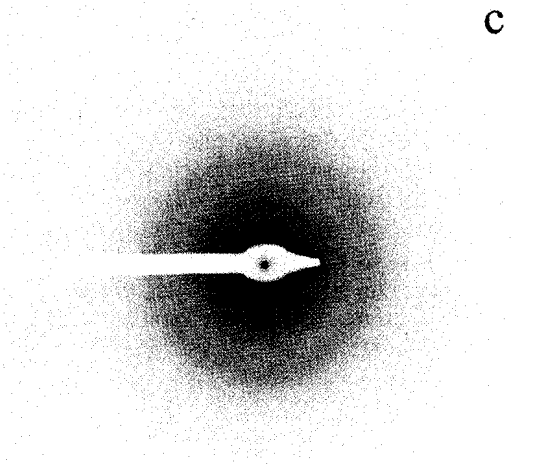

(~0.80 mg m^{-3}), whereas Atlantic and Frontal waters had less (~0.60 and 0.50 mg m^{-3}, respectively).

Vertical profiles of TOC were different from site to site and were not closely coupled to the Chl *a* content. Mediterranean waters had several TOC peaks; the 40-m peak was apparently the DCM. High TOC concentrations above 20 m might be due to contamination or poor response of the analyzer to particle-rich water because the TOC samples were not filtered. Two TOC peaks at 5 and 40 m marked Frontal waters, and seemed tightly coupled to Chl *a*. Atlantic waters contained only one TOC peak (at 20 m) and were not coupled to Chl *a*.

Quantification of the three organic matter pools (dissolved, colloidal, particulate)—Concentrations and percentages of organic carbon in the different size fractions are listed in Table 2. In all water masses and at both 5 and 40 m deep, 60–0.2-µm organic particles accounted for only 6–9% of the TOC. Organic colloids (included in the 0.2-µm to 1,000-Da fraction) accounted for 1–12% of TOC. The DOC fraction (<1,000 Da) made up 80% of TOC. No clear relationship between TOC concentrations and organic colloidal percentages could be seen. The highest percentage of TOC in colloids was found where TOC was high (40 m deep).

In the Almeria–Oran Front system, the colloidal organic pool was low and there was little difference between the sites studied. COC has been observed to decrease from fresh to coastal to open ocean waters, implying that terrestrial inputs could be an important source of colloidal organic matter (Sempéré et al. 1994; Guo et al. 1995). However, our salinity data indicate that in the AOF area, terrestrial inputs were probably limited. On the other hand, marine sources such as phytoplankton or degraded particles may also contribute significantly to the COC pool (Guo and Santschi 1997 and references therein; Sempéré et al. 2000*a*). The colloidal organic material may be low because (1) its production is strongly dependent on the biological activity that follows a seasonal pattern or (2) the COC is quickly cycled by either biological activity or aggregation and sedimentation.

Morphological characterizations of the colloids—The colloid sizes observed on the TEM specimen grids ranged from 10 nm to 5 µm long. Colloid morphologies are shown in Figs. 3–5 and have been categorized into three main morphotypes: rounded globules (G), aggregates of rounded entities (RA), and spherulitic compact aggregates (SA). While the two first morphotypes are amorphous as shown by the microdiffraction picture, the third morphotype is crystalline.

Morphotype G, with diameters between 10 to 200 nm (Fig. 3a,b) were composed of no more than five smaller rounded entities (e) having on average a diameter of 30 nm

←

Fig. 4. (a) TEM images of aggregates of rounded entities (RA). (b) Note the difference in the aggregation structure between linear (Lp) and compact (Cp) parts. (c) Typical microdiffraction picture of the rounded aggregates.

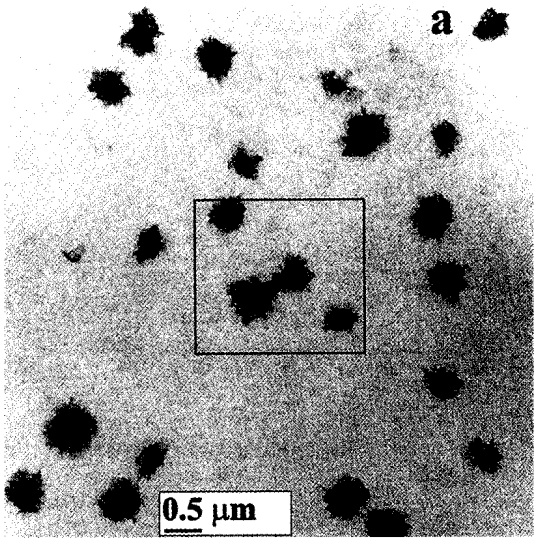

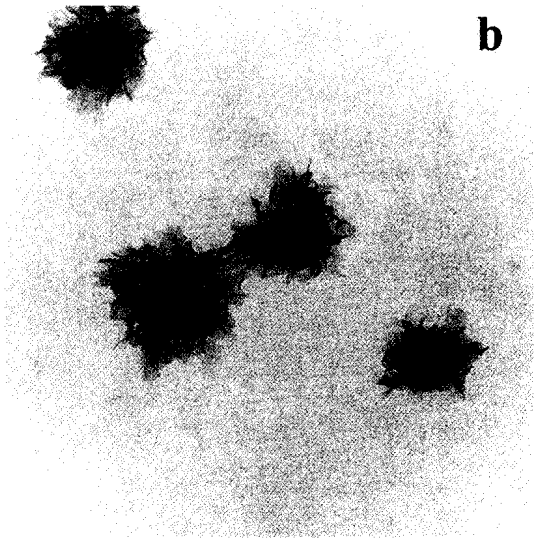

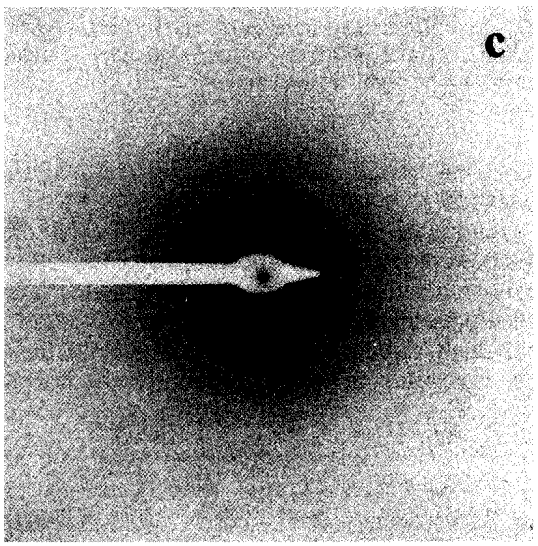

Table 3. Relative abundance of the different colloidal morphologies encountered in the Almeria–Oran Front System (+++ high; + low; − not observed).

	Globules	Aggregates of rounded entities	Spherulitic aggregates
Mediterranean waters			
5 m	+++	+	−
40 m	+	+++	+
Frontal waters			
5 m	+++	−	−
40 m	+++	+	−
Atlantic waters			
5 m	+++	−	−
40 m	+	−	+++

(Fig. 3b). Some of the globules aggregated linearly to become chainlike, as observed in Fig. 3a.

The second morphotype RA included aggregates made up of more than 50 rounded entities with diameters ranging from 10 to 50 nm (Fig. 4a,b). Their structure was largely open and contained both linear parts (Lp) and compact parts (Cp) (Fig. 4b). Most of the aggregates we observed were larger than 200 nm despite being filtered through 200-nm pore size filters before TEM observations. This might be because of a flexible character or to aggregation after filtration.

The third morphotype SA, shown in Fig. 5a,b, was formed of crystalline needlelike entities approximately 30 nm wide and 150 nm long. Five diffraction rings were determined, corresponding to lattice spacing of 2.11, 1.48, 1.22, 0.93, and 0.87 Å (Fig. 5c).

The abundance of the different colloidal morphologies varied according to sampling site and water depth. At 5 m for all water types, the most abundant colloidal morphology was globules (Table 3). At 40 m, each water mass was characterized with a dominance of one morphotype: RA in Mediterranean waters, G in Frontal waters, and SA in Atlantic waters.

Chemical nature of the different morphotypes of colloids—Elemental analyses of the different colloidal morphotypes were performed using EDS. The characteristics of the detector we used did not permit measurement of elements with atomic number ≤ 11. Thus, the C and N contents, which are indicators of organic matter, could not be determined. The quantitative microchemical data were calculated using the Cliff and Lorimer (1975) method. Once the background was subtracted, EDS microanalyses of the different colloidal morphotypes gave a small total number of counts after 100 s of analysis. Values often ranged between 1 and 70 counts, which indicates in most cases that the colloids are organic.

←

Fig. 5. (a) and (b) Two different magnifications of TEM images of spherulitic aggregates as described in the text. (c) Typical microdiffraction picture of the spherulitic aggregates.

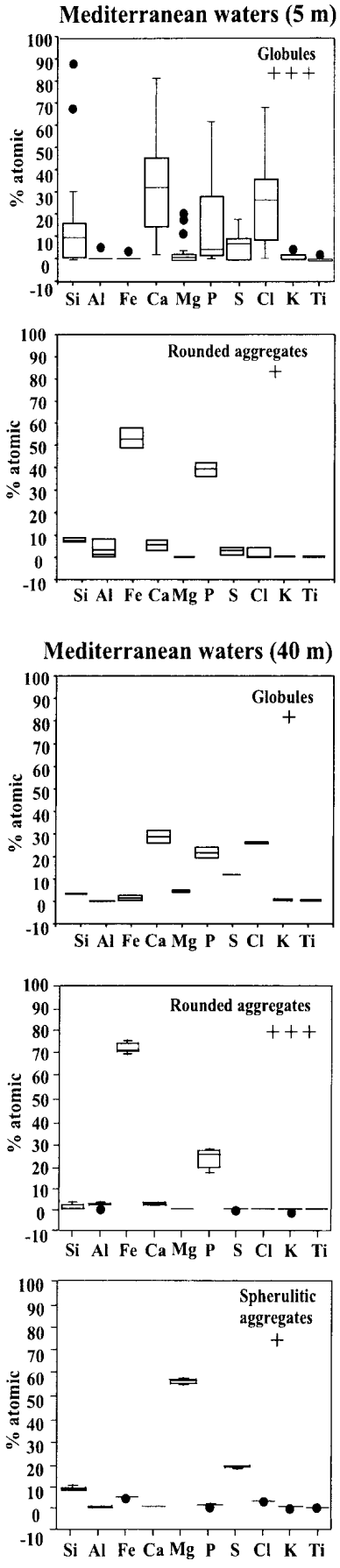

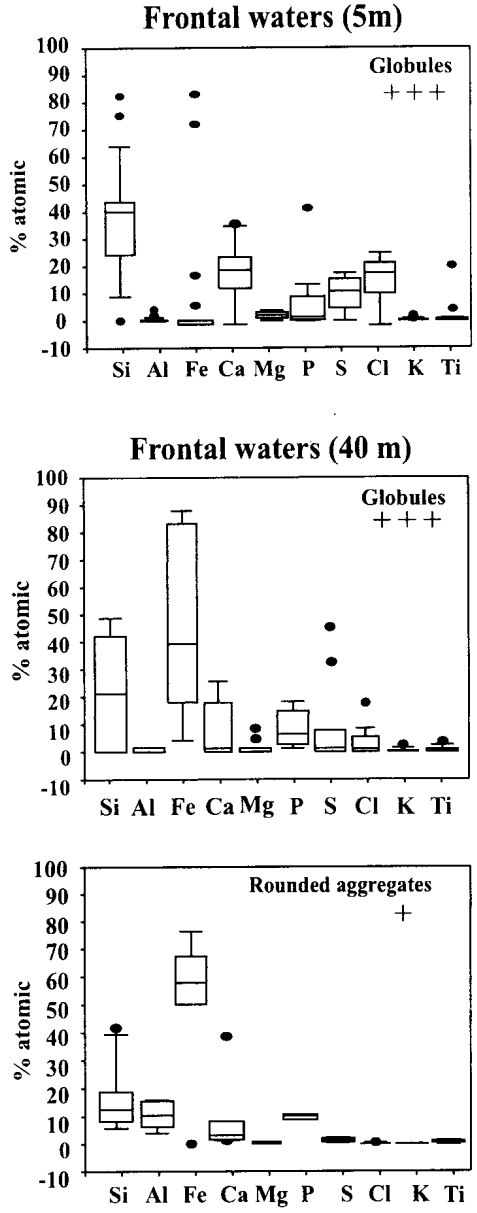

Fig. 7. Box plot representations of the chemical composition of the different colloidal morphotypes encountered in Frontal waters (abundance: +++ high, + low).

By comparison, under the same conditions of analysis, a clay particle would give around 1,000 counts.

Ten quantifiable elements (Si, Al, Fe, Ca, Mg, P, S, Cl, K, and Ti) were detected, indicating the complexity of the chemical composition of the colloids. Figures 6, 7, and 8 are box plot representations of the percentages of each element detected. Such representations give a general idea of the chemical variability of each morphotype. Each box repre-

←

Fig. 6. Box plot representations of the chemical composition of the different colloidal morphotypes encountered in Mediterranean waters (abundance: +++ high, + low).

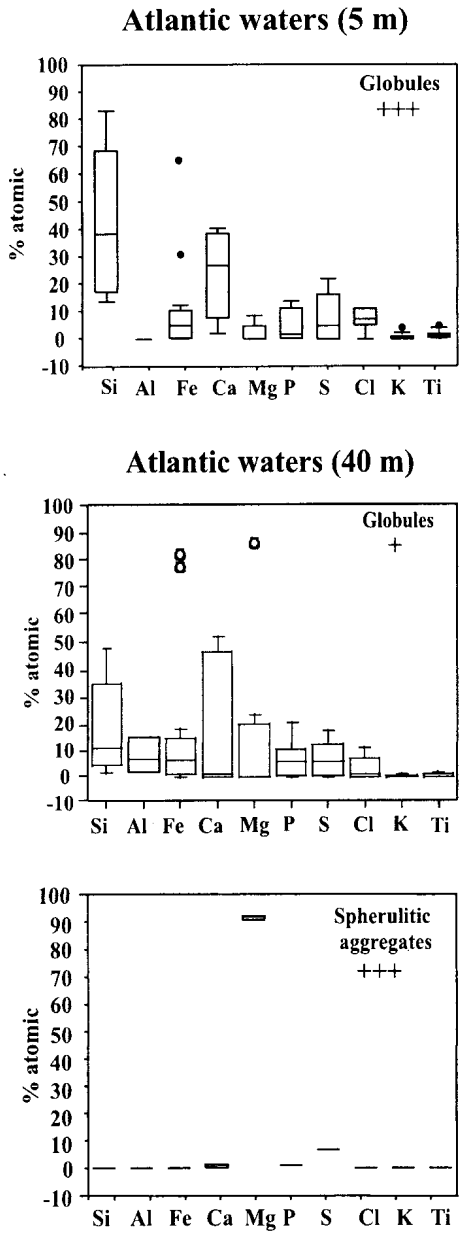

Fig. 8. Box plot representations of the chemical composition of the different colloidal morphotypes encountered in Atlantic waters (abundance: +++ high, + low).

sents values between the 25th and 75th percentiles. The line across the box indicates the median. Lines extending from the box mark the range of observed values inside the "inner fences." Any value outside of the defined range, called an outlier, is displayed as an individual black point.

Globules, at both depths (5 and 40 m) and in all three water types, had the most diversified chemical composition, with Si, Al, Fe, Ca, Mg, P, S, and Cl present. The range of values between the 25th and the 75th percentile was often greater than 10%, showing a high variability of each element content. Ca, P, S, and Cl were found in all the globules. However, differences were noted between water masses, particularly the high concentration of Si (median 40%) and Fe (median 40%) for Frontal globules at 5 and 40 m, respectively, and a high concentration of Mg in Atlantic globules. By contrast, morphotype RA was less variable. In Mediterranean waters, RA had high content of Fe (≥50%) and P (≥30%) and a high content of Fe (~60%) and some Si, Al, Ca, and P in Frontal waters. Although great care was taken during handling, contamination by P and Fe cannot be ruled out because the membrane was cleaned with H_3PO_4 in addition to NaOH and Milli-Q water, possibly inducing P contamination. In addition, Fe contamination could have occurred during sampling. The SA morphotype, found mainly in Atlantic waters at 40 m, was chemically the most homogeneous, magnesium being the predominant element (≥60%).

The globule morphotypes we observed in the three water masses of the AOF seemed to be similar to those seen in coastal and shelf waters off California by Wells and Goldberg (1991, 1994), who suggested that the globules, because of their low opacity to electrons and their granular structure, were composed mainly of organic matter, although they also contained some trace metals such as Fe, Co, Si, and Al. These authors hypothesized that globules are formed from an aggregation of organics of relatively low molecular weight. Such clear morphological and structural resemblance strongly suggests that our globule morphotypes could also be mainly organic matter transporting metals in variable quantities. The globule morphotypes may also originate from land-derived organic matter, which is more abundant in Mediterranean waters than in large oceans (Sempéré et al. 2000*b*). Mg-rich SA appear to have never been previously described in aquatic systems.

Aggregation and formation of colloids—Aggregation of particles >1 μm is relatively well known in marine waters and can result in marine snow formation, an increase in food availability for zooplankton, or changes in optical properties (Alldredge and Jackson 1995 and references therein). By contrast, aggregation and formation of marine colloidal material is little documented. Several authors have suggested that rates of colloid formation must be rapid, presumably because of a combination of cell exudation and lysis, microbial degradation of particulate organic matter (POM), and excretion by zooplankton (Koike et al. 1990). Wells and Goldberg (1993) suggested that one of the primary sources of marine colloids is the agglomeration of some fractions of the dissolved organic phase. Recently, Chin et al. (1998) demonstrated that marine polymer gels can assemble from free dissolved organic matter (DOM) polymers, transforming DOM into POM with the strong influence of cations such as Ca^{2+} and Mg^{2+}.

A common chemical characteristic of all the globules observed in this work is the presence of Ca. As demonstrated by Chin et al. (1998), this strongly suggests that Ca plays a role in globule formation, in the aggregation of the elementary entities constituting the globule, and in interactions between the globules themselves. The elemental composition of "pure plankton" is 11, 20.5, 68, 0.09, and 0.06% for P, Ca, Si, Al, and Fe, respectively (Martin et al. 1976). Colloids obtained by EDS are chemically similar with, on average, 11% P, 30% Ca, 35% Si, and 2% Al but with greatly enhanced Fe at 21%. This high percentage of Fe might be due to contamination, as

stated above. However, such similarity implies that degradation of plankton is important in globule production.

By contrast, rounded entity aggregates (mainly encountered in Mediterranean waters at 40 m) are rich in Fe and P and display an open, strongly linked structure characteristic of cluster–cluster diffusion-limited aggregation (DLA), as discussed in Senesi (1994). In such an aggregation process, movable clusters collide and stick together to form large clusters. Usually in that case, the fractal dimension is around 1.78. However fractal dimensions obtained on our aggregates were lower (1.44 and 1.73 with values around 1.22 and 1.82, respectively) for the linear and compact parts shown on Fig. 4b. Low values observed for linear parts deviate from a strict DLA process. Such low fractal dimensions have been already reported for lake aggregates by Zhang and Buffle (1996 and references therein) and were explained by probable polarization of hematite. In marine systems, Logan and Wilkinson (1990) calculated a fractal dimension of 1.39 ± 0.15 for all types of marine submicrometer aggregates (0.4–20 mm) and 1.52 ± 0.19 for large diatom aggregates (7–20 mm). Kilps et al. (1994) calculated a fractal dimension of 1.72 for marine snow particles (1–60 mm) using in-situ photographs. From our observations, it appears that low fractal dimensions for submicrometer aggregates are a general feature in marine systems.

References

ALLDREDGE, A. L., AND G. A. JACKSON. 1995. Aggregation in marine systems. Deep-Sea Res. II **42:** 1–7.

AMON, R. M. W., AND R. BENNER. 1994. Rapid cycling of high-molecular-weight dissolved organic matter in the ocean. Nature **369:** 549–552.

ARNONE, R. A., D. A. WIESENBURG, AND K. D. SAUNDERS. 1990. The origin and characteristics of the Algerian Current. J. Geophys. Res. **95:** 1587–1598.

BASKARAN, M., P. H. SANSTCHI, G. BENOIT, AND B. D. HONEYMAN. 1992. Scavenging of thorium isotopes by colloids in seawater of the Gulf of Mexico. Geochim. Cosmochim. Acta **56:** 3375–3388.

CHIN, W.-C., M. V. ORELLANA, AND P. VERDUGO. 1998. Spontaneous assembly of marine dissolved organic matter into polymer gels. Nature **391:** 569–571.

CLIFF, G., AND G. W. LORIMER. 1975. The quantitative analysis of thin specimens. J. Microsc. **103:** 203–207.

DAFNER, E., R. SEMPERE, N. GONZALES, F. GOMEZ, AND M. GOUTX. 1999. Cross slope variations of dissolved organic carbon in the Gulf of Cadiz, NE Atlantic Ocean (February, 1998). Mar. Ecol. Prog. Ser. **189:** 301–306.

FRÖSCH, D., AND C. WESTPHAL. 1989. Melanine resins and their application in electron microscopy. Electron Microsc. Rev. **2:** 231–255.

GROUT, H., AND C. PARRON. 1997. Mise en évidence de silice à l'état colloïdal dans des cours d'eau d'Amazonie (Evidence of colloidal silica in Amazonian streamwaters). C. R. Acad. Sci. Paris **324**(sér. IIa): 747–752.

———, M. R. WIESNER, AND J.-Y. BOTTERO. 1999. Analysis of colloidal phases in urban stormwater runoff. Environ. Sci. Technol. **33:** 831–839.

GUO, L., AND P. H. SANTSCHI. 1997. Composition and cycling of colloids in marine environments. Rev. Geophys. **35:** 17–40.

———, P. H. SANTSCHI, AND K. W. WARNKEN. 1995. Dynamics of dissolved organic carbon (DOC) in oceanic environments. Limnol. Oceanogr. **40:** 1392–1403.

KILPS, J. R., B. E. LOGAN, AND A. L. ALLDREDGE. 1994. Fractal dimensions of marine snow aggregates determined from image analysis of in situ photographs. Deep-Sea Res. I **41:** 1159–1169.

KOIKE, I., H. SHIGEMITSU, T. KAZUKI, AND K. KAZUHIRO. 1990. Role of sub-micrometer particles in the ocean. Nature **345:** 242–244.

LEPPARD, G. G. 1997. Colloidal organic fibrils of acid polysaccharides in surface waters: Electron-optical characteristics, activities and chemical estimates of abundance. Colloids Surf. A: Physicochem. Eng. Asp. **120:** 1–15.

———, A. HEISSENBERGER, AND G. J. HERNLD. 1996. Ultrastructure of marine snow. I. Transmission electron microscopy methodology. Mar. Ecol. Prog. Ser. **35:** 289–298.

———, M. M. WEST, D. T. FLANNINGAN, J. CARSON, AND J. N. A. LOTT. 1997. A classification scheme for marine organic colloids in the Adriatic Sea: Colloid speciation by transmission electron microscopy. Can. J. Fish. Aquat. Sci. **54:** 2334–2349.

LOGAN, B. E., AND D. B. WILKINSON. 1990. Fractal geometry of marine snow and other biological aggregates. Limnol. Oceanogr. **35:** 130–136.

MARTIN, J. H., K. W. BRULAND, AND W. W. BROENKOW. 1976. Cadmium transport in the California Current, p. 159–184. *In* H. Windom and R. Duce [eds.], Marine pollutant transfer. Health Lexington.

MORAN, S. B., P. A. YEATS, AND P. W. BALLS. 1996. On the role of colloids in trace metal solid-solution partitioning in continental shelf waters: A comparison of model results and field data. Cont. Shelf Res. **16:** 397–408.

PRIEUR, L., AND A. SOURNIA. 1994. Almofront 1: An interdisciplinary study of the Almeria Oran geostrophic front, SW Mediterranean Sea. J. Mar. Syst. **5:** 187–204.

SANTSCHI, P., E. BALNOIS, K. J. WILKINSON, J. ZHANG, J. BUFFLE, AND L. GUO. 1998. Fibrillar polysaccharides in marine macromolecular organic matter as imaged by atomic force microscopy and transmission electron microscopy. Limnol. Oceanogr. **43:** 896–908.

SEMPÉRÉ, R., G. CAUWET, AND J. RANDON. 1994. Ultrafiltration of seawater with a zirconium and aluminum oxide tubular membrane: Application to the study of colloidal organic carbon distribution in an estuarine bottom nepheloid layer. Mar. Chem. **46:** 49–60.

———, S. C. YORO, F. VAN WAMBEKE, AND B. CHARRIERE. 2000*a*. Microbial decomposition of large organic particles in northwestern Mediterranean Sea. Mar. Ecol. Prog. Ser. **198:** 61–72.

———, B. CHARRIERE, F. VAN WAMBEKE, AND G. CAUWET 2000*b*. Carbon inputs of the Rhône River to the Mediterranean Sea: Biogeochemical implications. Glob. Biogeochem. Cycles **14:** 669–681.

SENESI, N. 1994. The fractal approach to the study of humic substances, p. 3–41. *In* N. Senesi and T. M. Miano [eds.], Humic substances in the global environment and implications on human health. Elsevier.

TENCE, M., J. P. CHEVALIER, AND R. JULLIEN. 1986. On the measurement of the fractal dimension of aggregated particles by electron microscopy: Experimental method, corrections and comparison with numerical models. J. Physique **47:** 1989–1998.

VIDEAU, C., A. SOURNIA, L. PRIEUR, AND M. FIALA. 1994. Phytoplankton and primary production characteristics at selected sites in the geostrophic Almeria-Oran front system. J. Mar. Syst. **5:**235–250.

WEITZ, D. A., AND J. S. HUANG. 1984. Self-similar structures and the kinetics of aggregation of gold colloids, p. 19–28. *In* F.

Family and D. P. Landau [eds.], Proceedings of the international topical conference on kinetics of aggregation and gelation, Athens, Georgia. North-Holland Elsevier Sci. Pub., Amsterdam.

WELLS, M. L., AND E. D. GOLDBERG. 1991. Occurrence of small colloids in sea water. Nature **353:** 342–344.

———, AND ———. 1993. Colloid aggregation in seawater. Mar. Chem. **41:** 353–358.

———, AND ———. 1994. The distribution of colloids in the North Atlantic and Southern Oceans. Limnol. Oceanogr. **39:** 286–302.

WILKINSON, K. J., S. STOLL, AND J. BUFFLE. 1995. Characterization of NOM–colloid aggregates in surface waters: Coupling transmission electron microscopy staining techniques and mathematical modelling. Fresenius J. Anal. Chem. **351:** 54–61.

———, A. JOZ-ROLAND, AND J. BUFFLE. 1997. Different roles of pedogenic fulvic acids and aquagenic biopolymers on colloid aggregation and stability in freshwaters. Limnol. Oceanogr. **42:** 1714–1724.

ZHANG, J., AND J. BUFFLE. 1996. Multi-method determination of the fractal dimension of hematite aggregates. Colloids Surf. A: Physicochem. Eng. Asp. **107:** 175–187.